Supplemental Information

High Performance Zn Anodes Enabled by a Multifunctional Biopolymeric Protective Layer for Dendrite-Free Aqueous Zinc-based battery

Lingzhi Kang,[ab] Jiale Zheng,[b] Huadong Yuan,[b] Jianmin Luo,[b] Yao Wang,[b] Yujing Liu,[b] Jianwei Nai,[b] Xinyong Tao*[b]

[a] Ecology and Health Institute, Hangzhou Vocational & Technical College, Hangzhou 310018, China

[b] College of Materials Science and Engineering, Zhejiang University of Technology, Hangzhou 310014, China. E-mail: tao@zjut.edu.cn

1. Experimental section

1.1. Preparation process

The commercial Zn foil was carefully polished with sandpaper to remove the passivation layer and cleaned up with deionized water and ethyl alcohol. Chitosan and Gelatin were dissolved in 2% acetic acid solution and aqueous solution, respectively. Subsequently, chitosan and gelatin were mixed together in a certain proportion under the condition of constant stirring at 60℃, and kept the temperature for 4h named as CG. After defoaming, coated the mixture to the zinc foil evenly. The modified Zn foil was dried at 60 ℃ for 6 h in a vacuum oven which is named as CG@Zn. As a comparison, the Zn foil coated with chitosan is named as C@Zn. A mixture of commercial V_2O_5, acetylene black, and PVDF binder in a mass ratio of 7:2:1 with appropriate amount of NMP were created to be a well-dispersed coating slurry. The slurry was cast on titanium foils via the doctor blade method and then dried at 60 ℃ for 12 h in a vacuum oven to be cathode material.

1.2. Materials Characterization

The exploration of phase structure was characterized through the X-ray diffraction

analysis (XRD, Ultima IV, Japan) with Cu-Kα (λ= 1.540598 Å, Smart Lab) source (scan rate of 5 $^{o}min^{-1}$). The micromorphology of the samples was observed using scanning electron microscopy (SEM, Nova NanoSEM 450, USA) equipped with corresponding energy dispersive spectroscopy (EDS) elemental mapping and atomic force microscope (AFM, Edge Dimension, USA). Atomic scale information of materials was obtained by transmission electron microscope (TEM, Talos-S, USA). The surface element analysis of the samples was carried out by a PHI 5000 VersaProbe XPS instrument (XPS, Axis Ultra DLD, Japan). The chemical structure was studied by Fourier transform infrared spectrum (FTIR, V80, USA). The concentration of Zn ions was measured using inductively coupled plasma-mass spectrometry (ICP-MS) with Thermo ICAP PRO.

1.3. Electrochemical Tests

Zn symmetrical cells were assembled in 1 M $ZnSO_4$ electrolyte by using 2032-type coin-cells in the air atmosphere. Electrochemical impedance spectroscopy (EIS) of the cell was recorded on an electrochemical workstation (CHI660E, Shanghai, China) over the frequency range of 100 kHz to 0.01 Hz. The electrodeposition test was conducted by using the treated Zn foil as the working electrode, platinum (Pt) wire as the counter electrode and Ag/AgCl as the reference electrode, respectively. The hydrogen evolution performance was recorded by linear voltammetry scanning (LSV) with a potential range of -1.0~-1.55 V vs. Ag/AgCl at a scan rate of 1 mV s^{-1}. The corrosion Tafel plot was measured through LSV with a potential range of -1.25~-0.65 V vs. Ag/AgCl at a scan rate of 10 mV s^{-1}. The diffusion curves were tested by chronoamperometry method under an overpotential of -150 mV.

Galvanostatic charge/discharge cycling was performed on the Neware battery tester. The Coulombic efficiency (CE) of the cell was evaluated at the current density of 1 mA cm^{-2} and 2 mA cm^{-2}, respectively. The performance of the full batteries was carried out in the voltage range of 0.2–1.6 V vs. Zn/Zn^{2+}. All obtained capacities were calculated based on the active mass of V_2O_5 cathode.

The ionic conductivity of samples was measured by using two blocking electrodes

(Ti foil) for the electrochemical impedance spectroscopy (EIS) measurement with an amplitude of 10 mV over a frequency from 100 kHz to 1 Hz at room temperature. The ionic conductivity was evaluated according to the following equation:

$$\sigma = \frac{L}{R_b S} \quad (1)$$

where R_b represents the resistance according to the EIS measurement, L represents the thickness of the sample and S is the contact area.

The transference number of Zn^{2+} ($t_{Zn^{2+}}$) was calculated by the following equation:

$$t_{Zn^{2+}} = \frac{Is\ (\Delta V\ -\ I_0 R_0)}{I_0(\Delta V\ -\ Is\ Rs)} \quad (2)$$

where ΔV represents the applied voltage (25 mV); I_0 and R_0 represent the initial current and resistance, respectively; I_s and R_s represent the steady-state current and resistance, respectively.

2. Figures and Tables

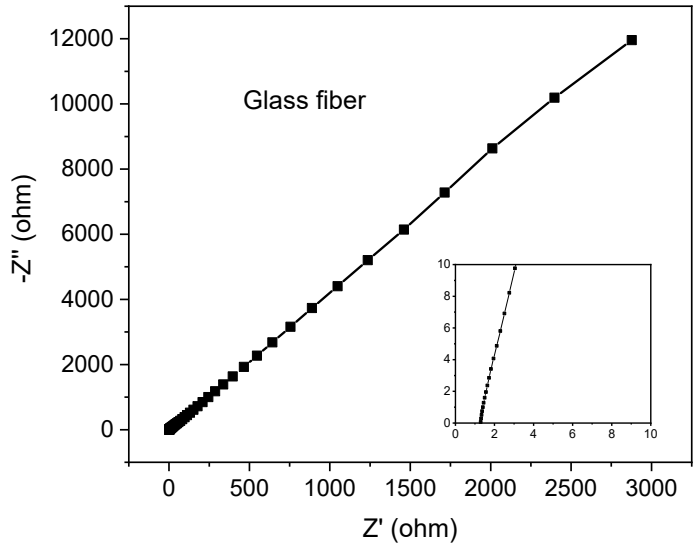

Fig. S1 Nyquist plots tested at open circuit voltage (OCV) over the frequency range of 100 kHz to 1 Hz with Ti symmetric cell with glass fiber as separator (inset: enlargement of indicated range).

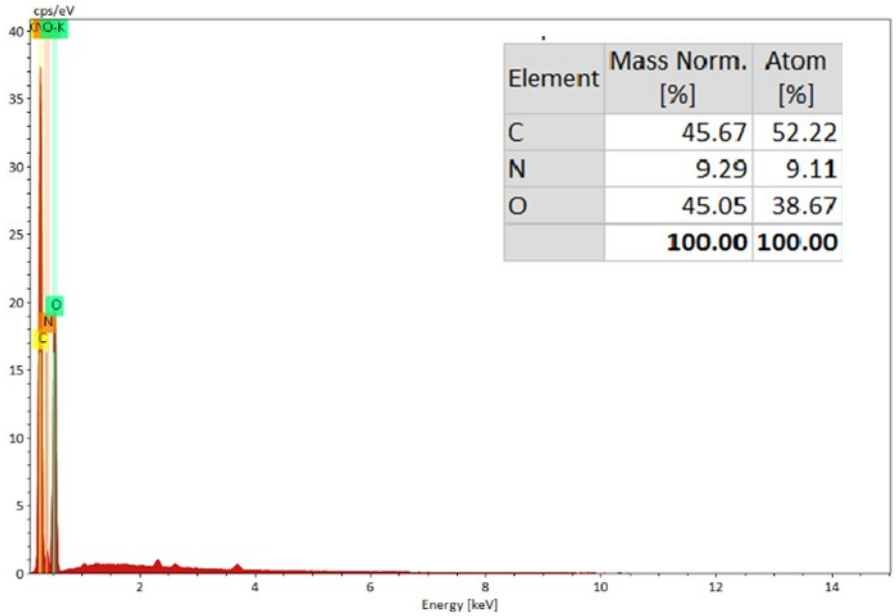

Element	Mass Norm. [%]	Atom [%]
C	45.67	52.22
N	9.29	9.11
O	45.05	38.67
	100.00	**100.00**

Fig. S2 EDS image of CG film (inset: the element content of CG).

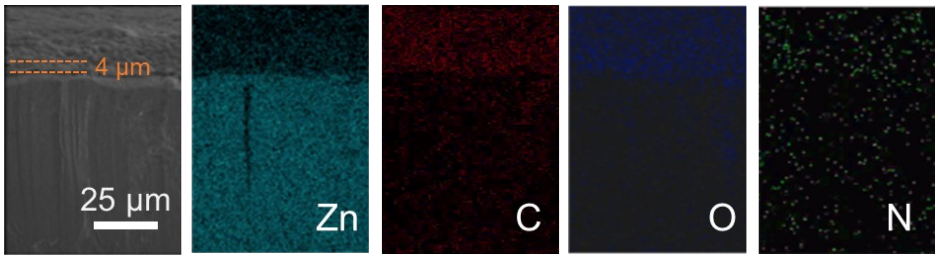

Fig. S3 Cross-sectional SEM image of CG@Zn foil and the corresponding element mappings of Zn, C, O, and N.

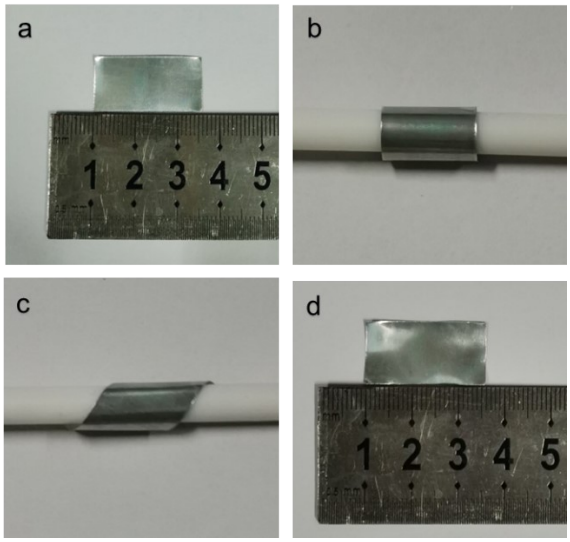

Fig. S4 Rolling and twisting experiments: (a) Photograph of the initial CG@Zn foil. (b and c) The rolling and twisting experiments. (d) Photograph of CG@Zn foil after rolling and twisting experiments.

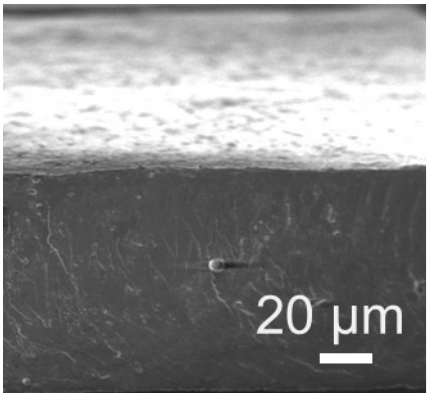

Fig. S5 SEM image of CG@Zn foil after rolling and twisting experiments.

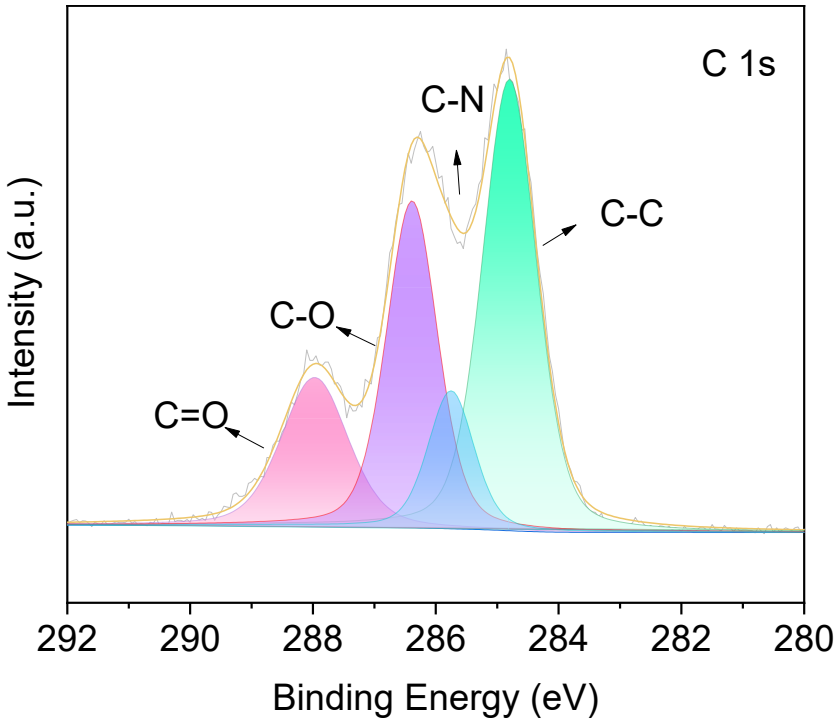

Fig. S6 The high-resolution XPS spectra of C 1s regions of CG film.

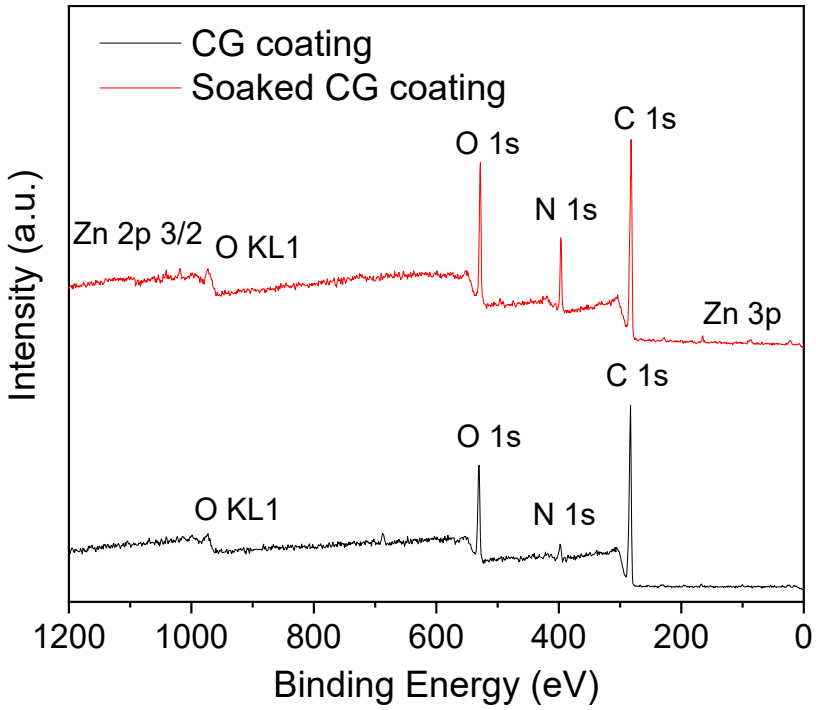

Fig. S7 X-ray photoelectron spectra (XPS) of CG and soaked CG.

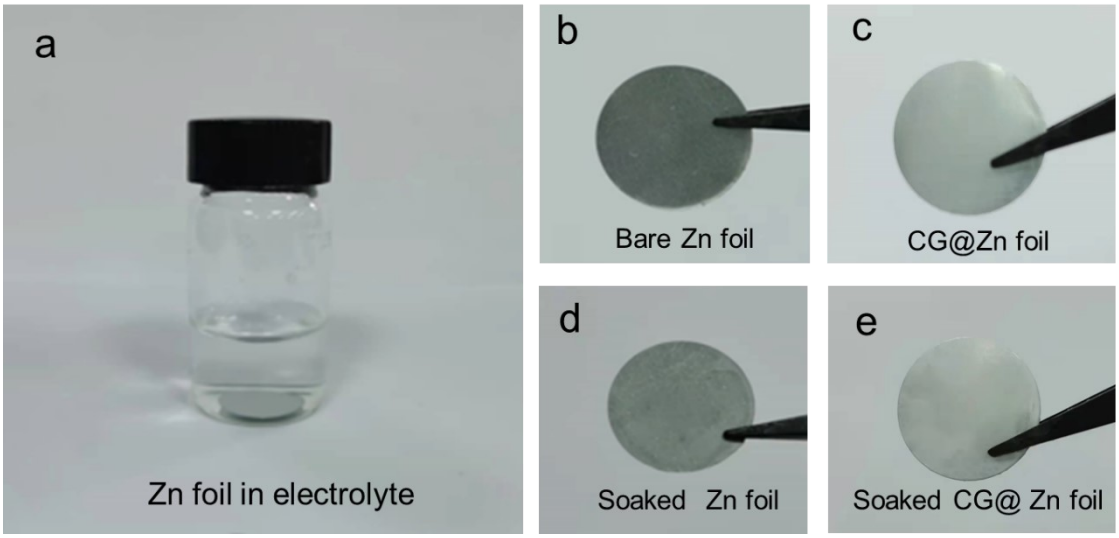

Fig. S8 (a) Zn foil soaked in 1 M $ZnSO_4$ electrolyte. (b, c) Digital images of the bare Zn and CG@ Zn foil. (d, e) Digital images of bare Zn and CG@Zn foil after soaking in electrolyte for 7 days.

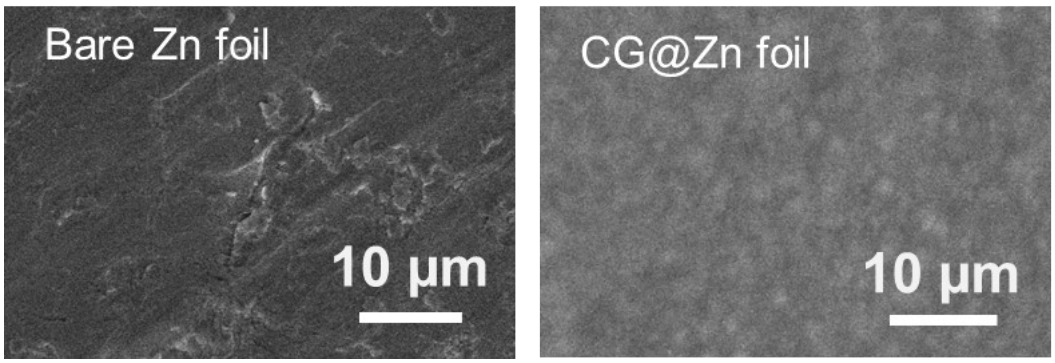

Fig. S9 SEM images of bare Zn foil and CG@Zn foil.

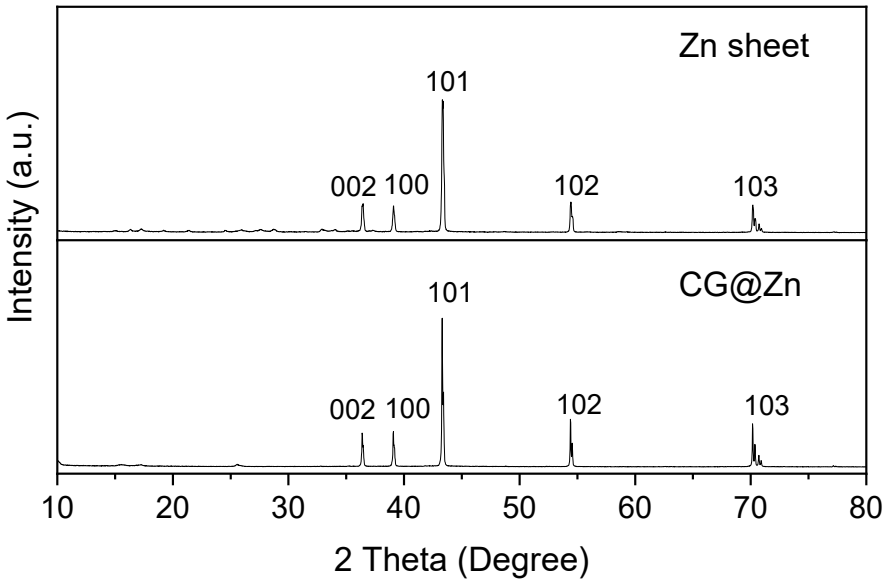

Fig. S10 XRD patterns of bare Zn sheet and CG@ Zn foil.

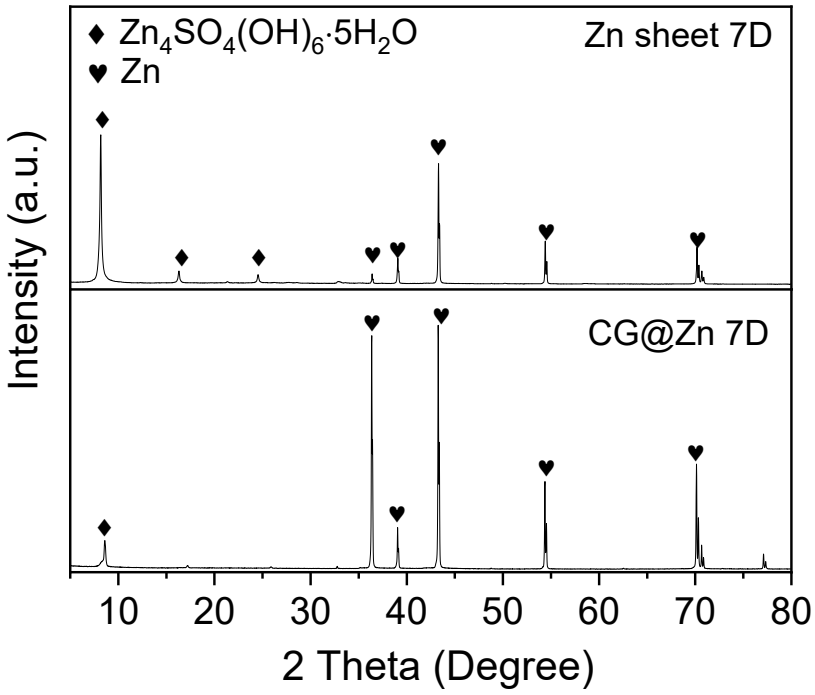

Fig. S11 XRD patterns of bare Zn sheet and CG@ Zn foil after soaking in 1 M $ZnSO_4$ for 7 days.

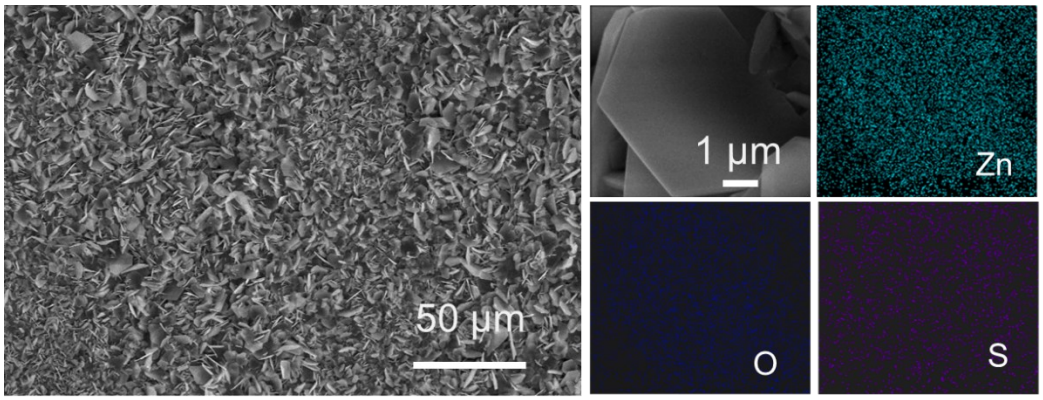

Fig. S12 SEM and EDS mapping images of bare Zn foil soaked in 1 M $ZnSO_4$ electrolyte.

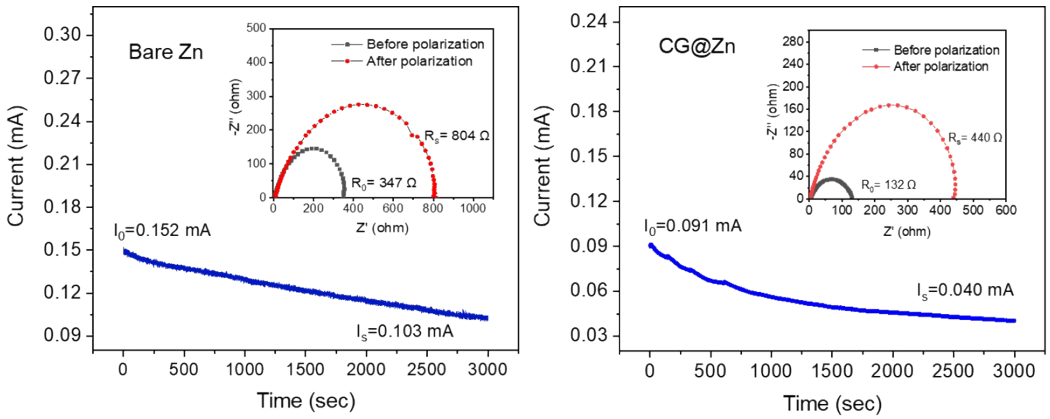

Fig. S13 Current-time plots of the bare Zn symmetric cell and CG@Zn symmetric cell after the application of a constant potential (inset: the impedance spectra before and after polarization).

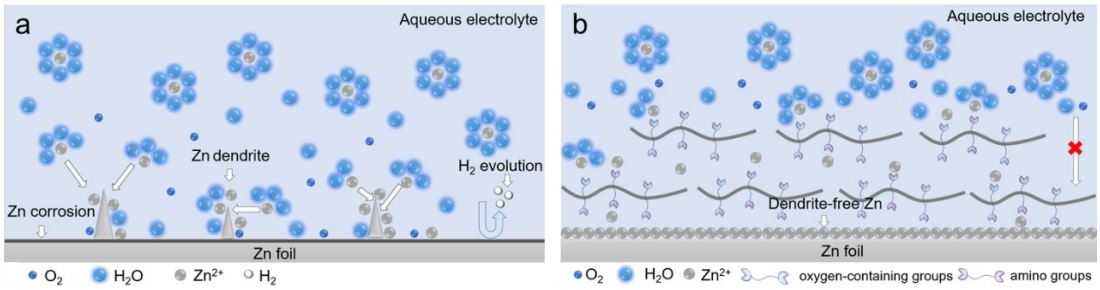

Fig. S14 Schematic diagram for Zn deposition on the bare Zn and CG@Zn.

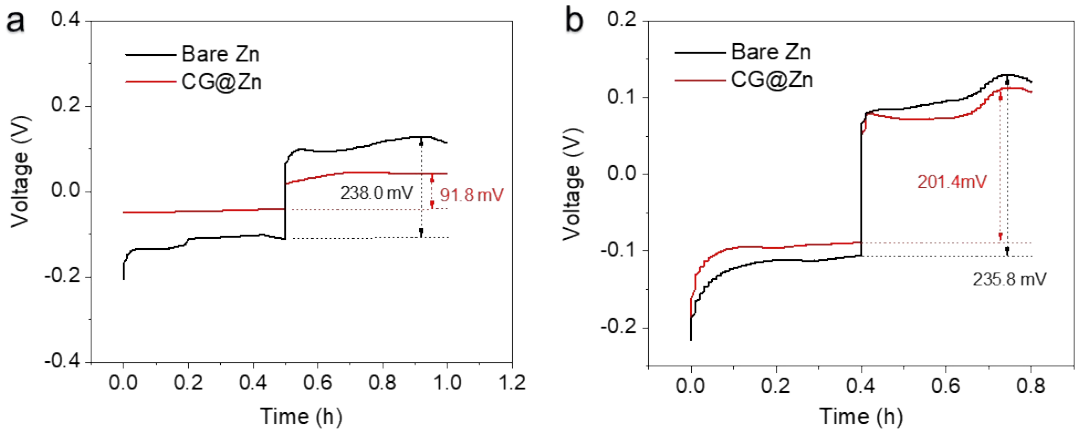

Fig. S15 (a) High-resolution voltage profiles at 2 mA cm^{-2} with the capacity of 1 mAh cm^{-2} for the first cycle. (b) High-resolution voltage profiles at 5 mA cm^{-2} with the capacity of 2 mAh cm^{-2} for the first cycle.

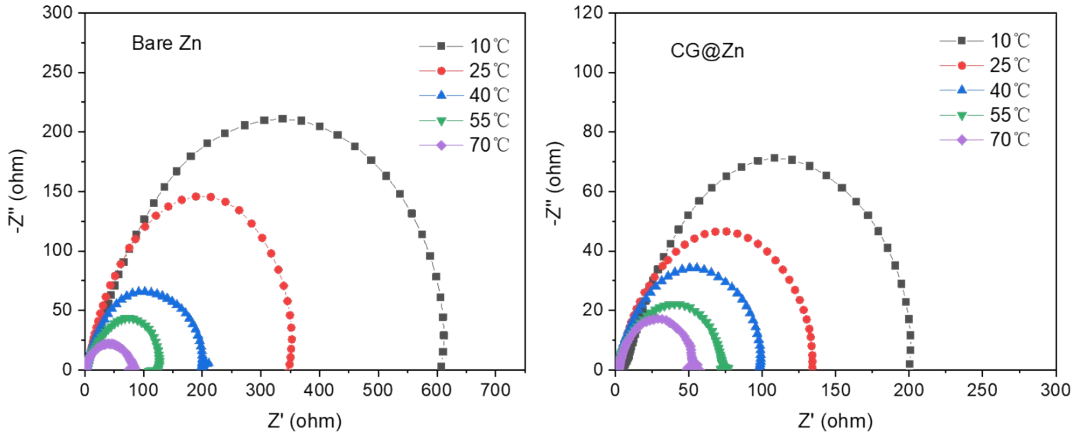

Fig. S16 Electrochemical impedance spectra of Zn and CG@Zn anodes at 10 ℃,25 ℃, 40 ℃, 55 ℃, and 70 ℃.

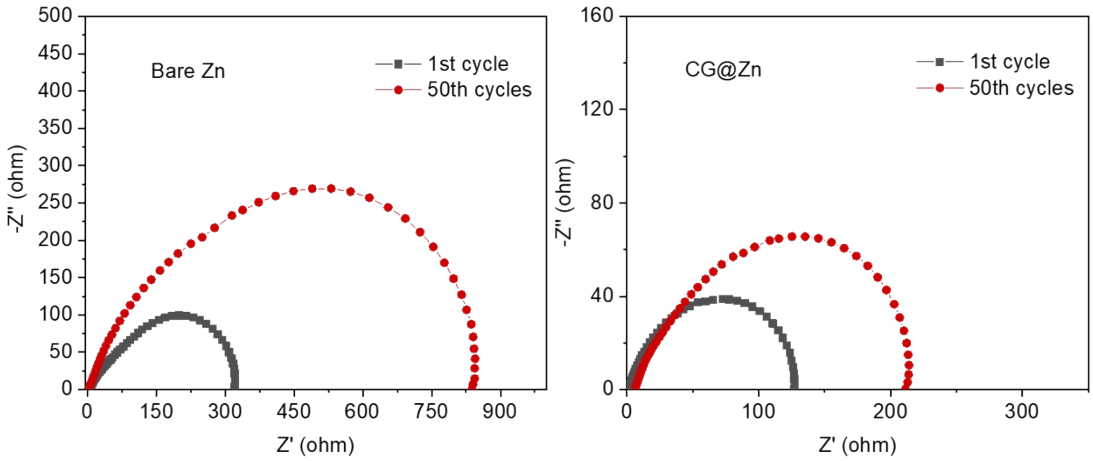

Fig. S17 Electrochemical impedance spectra of Zn and CG@Zn anodes at 1st and 50th cycles.

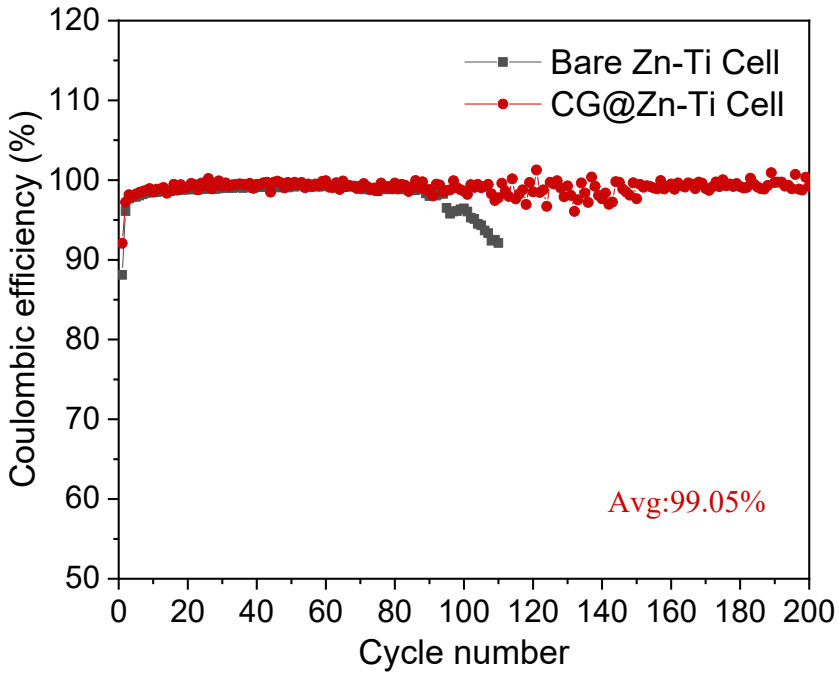

Fig. S18 CE of Zn plating/stripping in bare Zn-Ti and CG@Zn-Ti cells at a current density of 2 mA cm^{-2} with a capacity of 1 mAh cm^{-2}.

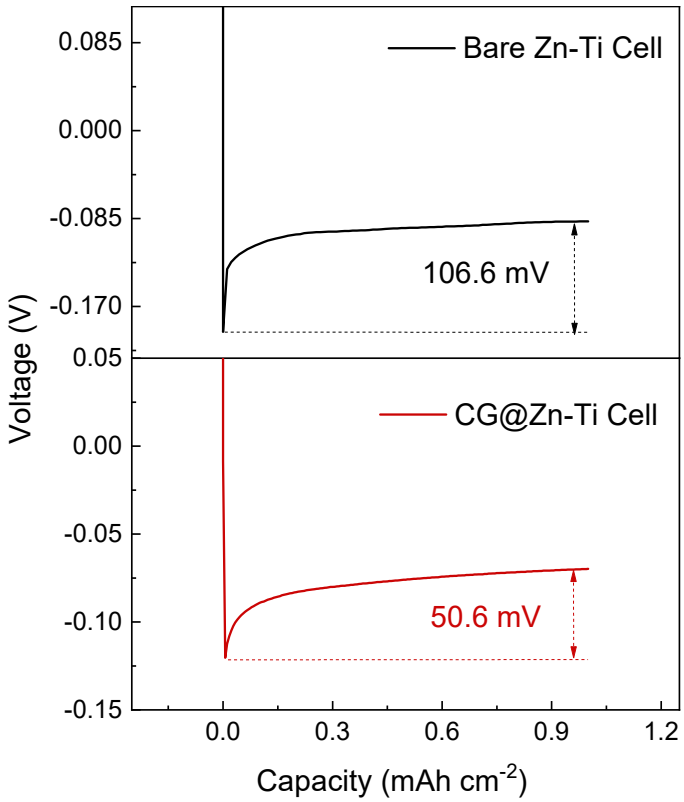

Fig. S19 Nucleation overpotential of bare Zn and CG@Zn asymmetric cells (versus Ti electrode) at 2 mA cm^{-2} for 1 mAh cm^{-2}.

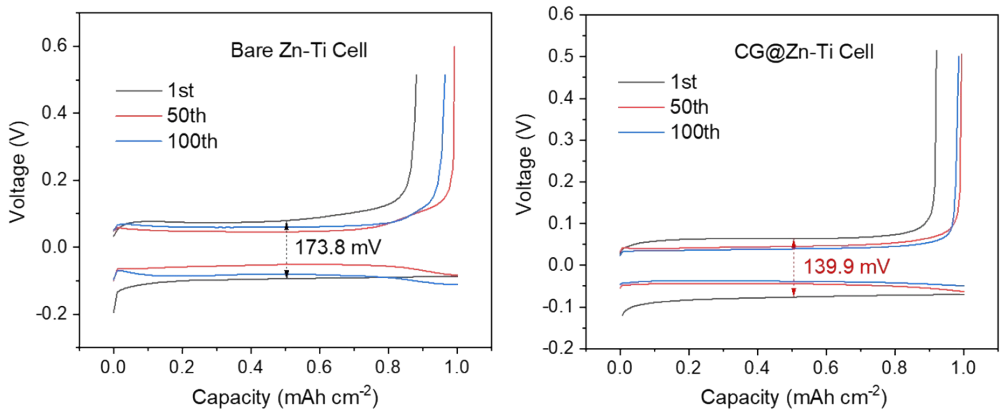

Fig. S20 Voltage profiles of bare Zn-Ti and CG@Zn-Ti cells after 1, 50, and 100 cycles at 2 mA cm^{-2} for 1 mAh cm^{-2}.

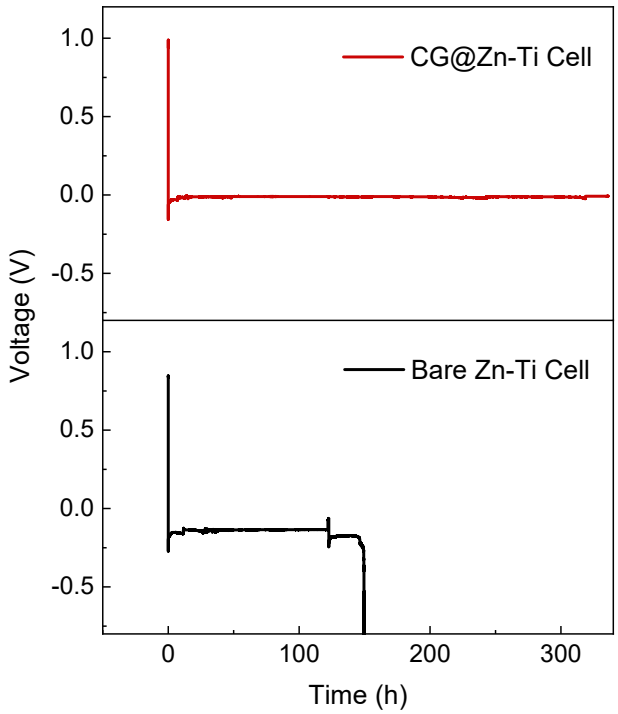

Fig. S21 The short-circuit test results of bare Zn-Ti and CG@Zn-Ti cells at the current density of 3 mA cm^{-2}.

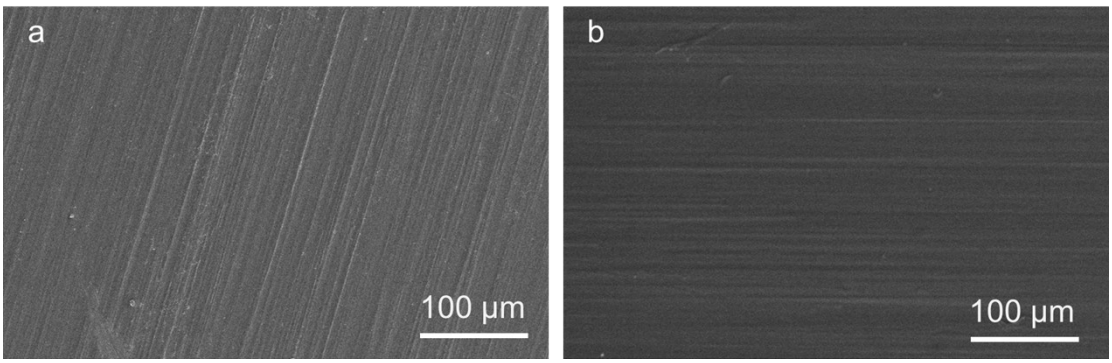

Fig. S22 SEM images of (a) Bare Ti foil and (b) CG coated Ti foil.

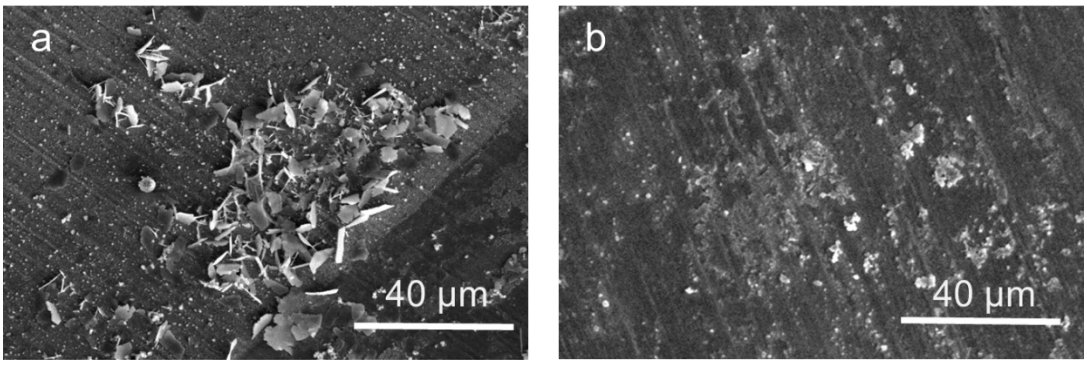

Fig. S23 SEM images of a) bare Ti electrode and b) CG@Ti electrode deposited zinc for 1 h.

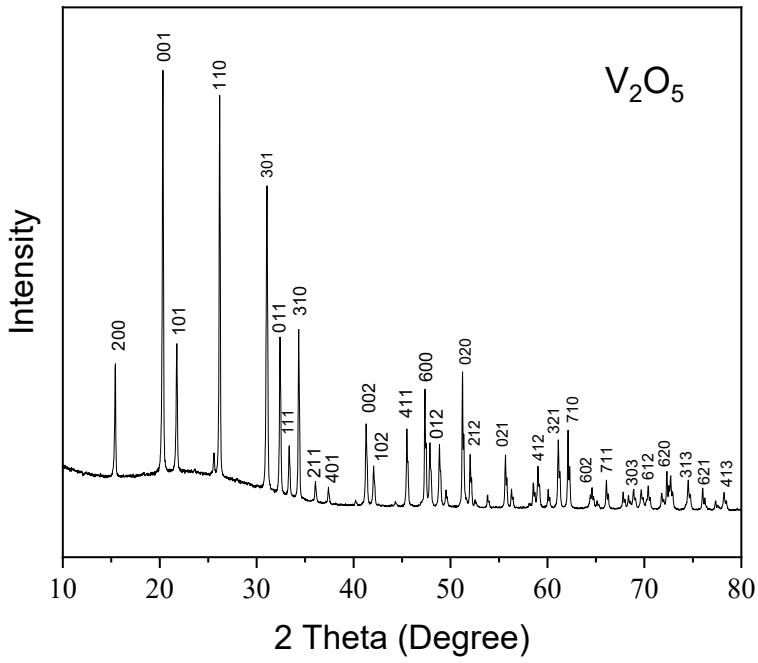

Fig. S24 XRD pattern of V_2O_5 cathode.

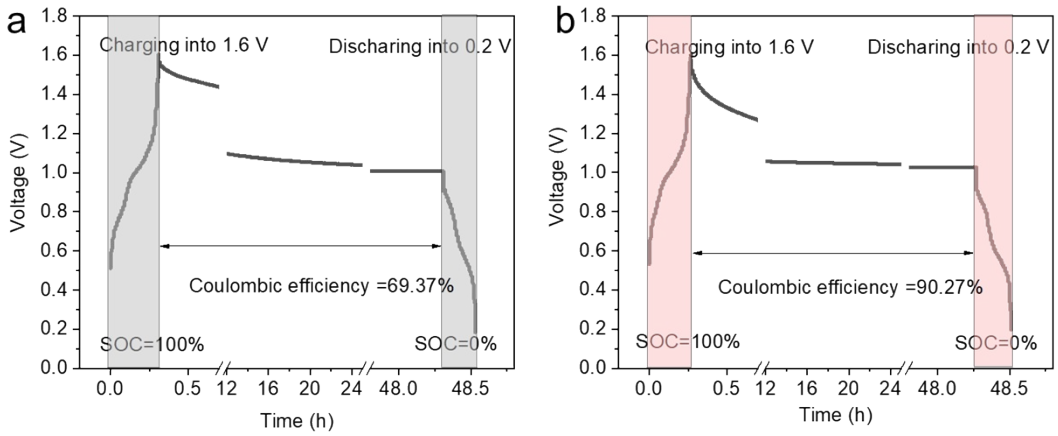

Fig. S25 (a) Bare Zn anode and (b) CG@Zn anode were first fully charged to 1.6 V, then the cells were rested at 100% stage of charge (SOC) for 48 h, followed by full discharging.

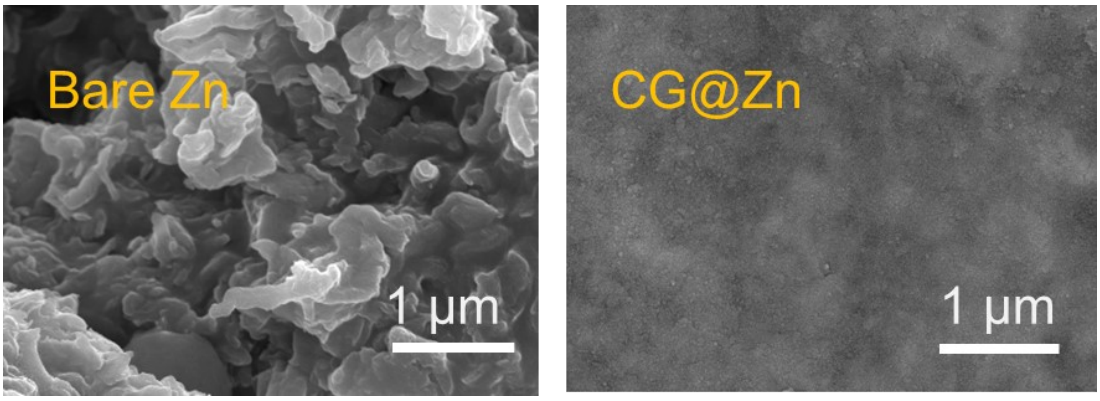

Fig. S26 Morphology images of full cells after cycling based on bare Zn and CG@Zn.

Table S1 Comparison of electrochemical performance of the different modified Zinc anodes for symmetric cells

Anode	Current density with capacity	Cycle life	Reference
Nano-$CaCO_3$ coating	0.25 mA cm^{-2} with 0.05 mA h cm^{-2}	400 h	[1]
Polyacrylonitrile layer	1 mA cm^{-2} with 1 mA h cm^{-2}	1145 h	[2]
Zif-67 layer	2 mA cm^{-2} with 1 mA h cm^{-2}	1200 h	[3]
Cyanoacrylate coating	2 mA cm^{-2} with 1 mA h cm^{-2}	400 h	[4]
β-PVDF coating	0.25 mA cm^{-2} with 0.05 mA h cm^{-2}	2000 h	[5]
MOF-PVDF coating	1 mA cm^{-2} with 0.5 mA h cm^{-2}	500h	[6]
In@Zn	2 mA cm^{-2} with 1 mA h cm^{-2}	900 h	[7]
3D-ZnO layer	5 mA cm^{-2} with 1.25 mA h cm^{-2}	500 h	[8]
Polyimide layer	4 mA cm^{-2} with 2 mA h cm^{-2}	300 h	[9]
$NaTi_2(PO_4)_3$ layer	1 mA cm^{-2} with 1 mA h cm^{-2}	260 h	[10]
CG layer	2 mA cm^{-2} with 1 mA h cm^{-2}	over 1200 h	This work

References

[1] L. Kang, M. Cui, F. Jiang, Y. Gao, H. Luo, J. Liu, W. Liang, C. Zhi, *Adv. Energy Mater.* 2018, **8**, 1801090.

[2] P. Chen, X. Yuan, Y. Xia, Y. Zhang, L. Fu, L. Liu, N. Yu, Q. Huang, B. Wang, X. Hu, Y. Wu, T. van Ree, *Adv. Sci.* 2021, **8**, 2100309.

[3] X. Liu, F. Yang, W. Xu, Y. Zeng, J. He, X. Lu, *Adv. Sci.* 2020, **7**, 2002173.

[4] Z. Cao, X. Zhu, D. Xu, P. Dong, M. O. L. Chee, X. Li, K. Zhu, M. Ye, J. Shen, *Energy Storage Mater.* 2021, **36**, 132.

[5] L. T. Hieu, S. So, I. T. Kim, J. Hur, *Chem. Eng. J.* 2021, **411**, 128584.

[6] M. Liu, L. Yang, H. Liu, A. Amine, Q. Zhao, Y. Song, J. Yang, K. Wang, F. Pan, *ACS Appl. Mater. Interfaces* 2019, **11**, 32046.

[7] P. Xiao, H. Li, J. Fu, C. Zeng, Y. Zhao, T. Zhai, H. Li, *Energy Environ. Sci.* 2022, **15**, 1638.

[8] N. Gogurla, A. K. Sinha, S. Santra, S. Manna, S. K. Ray, *Sci. Rep.* 2014, **4**, 6483.

[9] M. Zhu, J. Hu, Q. Lu, H. Dong, D. D. Karnaushenko, C. Becker, D. Karnaushenko, Y. Li, H. Tang, Z. Qu, J. Ge, O. G. Schmidt, *Adv. Mater.* 2021, **33**, 2007497.

[10]M. Liu, J. Cai, H. Ao, Z. Hou, Y. Zhu, Y. Qian, *Adv. Funct. Mater.* 2020, **30**, 2004885.